The Journal of Pathology: Clinical Research
J Pathol Clin Res July 2018; **4:** 184–192
Published online 14 April 2018 in Wiley Online Library (wileyonlinelibrary.com). DOI: 10.1002/cjp2.100

ORIGINAL ARTICLE

Vascularization of colorectal carcinoma liver metastasis: insight into stratification of patients for anti-angiogenic therapies

Anthoula Lazaris[1†*], Abdellatif Amri[1†], Stephanie K Petrillo[1], Paublo Zoroquiain[1], Nisreen Ibrahim[2], Ayat Salman[1], Zu-Hua Gao[3], Peter B Vermeulen[4] and Peter Metrakos[1,2]

[1] *Department of Surgery, McGill University Health Center Research Institute, Cancer Research Program, Quebec, Canada*
[2] *Department of Anatomy and Cell Biology, McGill University, Quebec, Canada*
[3] *Department of Pathology, McGill University Health Center, Quebec, Canada*
[4] *Translational Cancer Research Unit, GZA Hospitals St.-Augustinus, Wilrijk, Belgium*

**Correspondence to: Anthoula Lazaris, Department of Surgery, McGill University Health Center Research Institute, Cancer Research Program, Quebec, Canada. E-mail: anthoula.lazaris@mail.mcgill.ca*

[†]*Both authors contributed equally.*

Abstract

Current treatment for metastatic disease targets angiogenesis. With the increasing data demonstrating that cancer cells do not entirely rely on angiogenesis but hijack the existing vasculature through mechanisms such as co-option of existing blood vessels, identification of targets has become of utmost importance. Our study looks at the vasculature of chemonaïve and treated colorectal carcinoma liver metastases (CRCLMs) to obtain a basic understanding of the microvessel density, type of vasculature (mature versus immature), and correlation with histopathological growth patterns that demonstrate unique patterns of angiogenesis. We performed immunohistochemistry on chemonaïve sections of desmoplastic histopathological growth pattern (DHGP) and replacement histopathological growth patterns (RHGP) lesions with CD31 [endothelial cell (EC) marker] and CD34/Ki67 double staining, which denotes proliferating ECs. The CD31 stains demonstrated a lower microvascular CD31 +ve capillary density in the DHGP versus RHGP lesions; and integrating both immunostains with CD34/Ki67 staining on serial sections revealed proliferating vessels in DHGP lesions and co-option of mature existing blood vessels in RHGP lesions. Interestingly, upon treatment with chemotherapy and bevacizumab, the RHGP lesions showed no necrosis whereas the DHGP lesions had almost 100% necrosis of the cancer cells and in most cases there was a single layer of viable cancer cells, just under or within the desmoplastic ring. The survival of these cells may be directly related to spatial location and possibly a different microenvironment, which may involve adhesion to different extracellular matrix components and/or different oxygen/nutrient availability. This remains to be elucidated. We provide evidence that DHGP CRCLMs obtain their blood supply via sprouting angiogenesis whereas RHGP lesions obtain their blood supply via co-option of existing vasculature. Furthermore current treatment regimens do not affect RHGP lesions and although they kill the majority of the cancer cells in DHGP lesions, there are cells surviving within or adjacent to the desmoplastic ring which could potentially give rise to a growing lesion.

Keywords: hepatobiliary and pancreas; liver; colorectal; carcinoma computerized image analysis; immunocytochemistry

Received 28 December 2017; Revised 21 February 2018; Accepted 1 March 2018

No conflicts of interest were declared.

Introduction

Colorectal carcinoma (CRC) remains the second leading cause of cancer death in the western world [1]. Over 50% of CRC patients develop liver metastases (LM) and 90% will die from metastatic disease [2]. Surgical resection of colorectal carcinoma liver metastases (CRCLMs) remains the only therapy resulting in 5-year survival rates of up to 50% and offers the possibility of a cure [3]. Unfortunately, only 20% of the patients with CRCLM are eligible for liver resection. For the remaining 80% of patients with unresectable CRCLM, treatment goals include achieving disease control, prolonging survival, and palliation of symptoms.

One of the well-defined hallmarks of cancer is the capacity to promote new blood vessel formation, a

process called angiogenesis [4]. However, this concept has been recently challenged as increasing evidence demonstrates that tumours are able to progress without angiogenesis by exploiting pre-existing vessels, using co-option [5]. Importantly, vessel co-option has been implicated in mediating resistance to anti-angiogenics [anti-vascular endothelial growth factor (VEGF)] in preclinical models of glioblastoma [6], hepatocellular carcinoma [7], melanoma brain metastases [8], lung metastases [9] and glioblastoma patients [10,11] and is also supported by our work in patients with CRCLM [12]. The first angiogenic inhibitor to be approved by the U.S. Food and Drug Administration was an anti-VEGF humanized monoclonal antibody (Bevacizumab: Bev), in combination with chemotherapy and was demonstrated to increase overall survival (OS) in first line treatment of metastatic colorectal cancer [2]. Trials with bevacizumab in combination with modern chemotherapy (FOLFOX and FOLFIRI) have been able to show increased progression-free survival but no difference in OS. Furthermore, clinical trials assessing the benefit of adjuvant therapy demonstrated disease progression in the majority of patients.

As evidence accumulates that vessel co-option is important in tumour progression [5], it becomes important to fully characterize the vascularization of cancer cells. The liver vascular architecture is unique, characterized by a sinusoidal network of vessels. The sinusoids are lined with fenestrated endothelium that has no basement membrane (space of Disse) and stands off from the underlying hepatocytes allowing space for the plasma to interact with the hepatocytes and hepatic stellate cells (the pericytes of the liver) [13].

Vermeulen *et al* describe three distinct histopathological growth patterns (HGPs) in CRCLM, each associated with distinct patterns of angiogenesis, recruitment and activation of host cells, and local invasion and growth [14]. They have been designated (1) the **desmoplastic** HGP (DHGP) characterized by a desmoplastic stroma at the interface of the metastases and liver parenchyma and no direct contact between the tumour cells and the hepatocytes; (2) the **pushing** HGP (PHGP) where liver cell plates are pushed aside by the growing tumour and run in parallel with the circumference of the metastases at the tumour-liver parenchyma interface and (3) the **replacement** HGP (RHGP) where tumour cells are replacing parenchymal cells in the liver plates. These HGPs can be assessed reproducibly on an H&E section according to international guidelines [15]. Although these HGPs have been identified as early as 1987 and infiltrative tumours were shown to have a worse prognosis [16], the biological explanation for the existence of the different HGPs remains unknown although some hypotheses have been put forward [15,17,18]. We have recently reported [12] in CRCLMs resected from patients that: (a) vessel co-option was the predominant mechanism of vascularization in approximately 40% of the lesions we examined, (b) metastases that utilize vessel co-option responded poorly to chemotherapy + bevacizumab, (c) vessel co-option was more prevalent in patients who progressed following treatment with chemotherapy + bevacizumab, and (d) patients with metastases that utilized vessel co-option obtained less clinical benefit from chemotherapy + bevacizumab in terms of OS.

A number of studies [14,19] have evaluated the vascularity in CRCLMs from patients who received neo-adjuvant chemotherapy with or without bevacizumab and related these findings to the HGP of the LM. These studies however were focused on investigating the effect of treatment on viability and vascularization of LMs and did not characterize the type of vasculature (immature versus mature vessels) and the effect of treatment. The present study undertook to characterize and quantify the mechanisms of vascularity of CRCLM lesions, stratified by HGP and the effect of current treatment regimens.

Materials and methods

Standard protocol approvals, registrations, and patient consent

The study was done in accordance with the guidelines approved by McGill University Health Centre (MUHC) Institutional Review Board (IRB). Prior written informed consent was obtained from all the subjects to participate in the study (protocol: SDR-11-066).

Clinical data

This study included a total of 50 lesions from 50 patients. Resections were performed between November 2011 and July 2014. Clinical data were collected for each patient through the locally established hospital database and medical records. Included within the data are demographics, primary and metastatic disease characteristics, relevant laboratory results, chemotherapy and comorbidities. The median age of diagnosis was 63 (range 31–81) years. Rectal carcinoma accounted for 34% of the cases. Approximately two-thirds (64%) of the patients had synchronous

liver metastasis (developed metastasis within a year of diagnosing the primary tumour). Twenty lesions (11 DHGP and 9 RHGP) were chemonaïve, 10 lesions (5 DHGP and 5 RHGP) received chemotherapy, and 20 lesions (10 DHGP and 10 RHGP) received chemotherapy + bevacizumab, with an average of seven cycles (range 3–28). Estimated 1 and 3-year OS is 100 and 82.6%, respectively. Twenty-seven (54%) patients had recurrence in the liver, with estimated 1 and 3-year disease-free survival 49.9 and 44.4%, respectively (26.5 months mean follow up duration).

Tissue sample acquisition

Informed consent was obtained from all patients through the MUHC Liver Disease Biobank (LDB: MUHC research ethics board approved protocol). Surgical specimens were procured and released to the Biobank immediately after the pathologist's confirmation of carcinoma and surgical margins. All mouse LM samples (splenic injections of Lewis Lung, MC38, CT26 into their syngeneic mouse strain) were a kind gift from Dr. Pnina Brodt and their generation described elsewhere [20].

Immunohistochemical staining

Formalin-fixed paraffin-embedded (FFPE) human CRCLM resected blocks and mouse livers with metastatic disease (blocks provided by Dr. Pnina Brodt) were used for this study. Serial sections 4-μm thick were cut from each FFPE block, mounted on charged glass slides (Superfrost Plus; Fisher Scientific, Waltham, MA, USA), and baked at 60 °C for 1 h prior to staining. Hematoxylin and eosin (H&E)-stained sections were prepared from all cases for an initial histopathological assessment.

Immunohistochemical (IHC) staining was performed using the Ventana BenchMark LT fully automated machine (Ventana Medical System Inc. AZ, USA) and stained for CD31(1:10; Monoclonal Mouse Anti-Human CD31, clone JC70A, Dako);VEGFA (prediluted; Monoclonal Rabbit Anti-Human VEGFA, clone SP28, Abcam), alpha SMA1 (1:100; Monoclonal Mouse Anti-Human Smooth Muscle Actin, Clone 1A4, Dako), and the combination of Ki67 (1:400; Rabbit Anti-Human Ki67; Thermofisher) and CD34 (1:100; Monoclonal Mouse Anti-Human CD34, clone QBEnd-10, Dako) using extended antigen retrieval (CC1 buffer).

Histopathological analysis and scoring

Histopathology scoring of the growth patterns was performed using the consensus guidelines [15]. All slides were scanned at 40× magnification using the Aperio AT Turbo system.

We evaluated microvascular density (MVD) in all lesions by staining with CD31, an endothelial cell (EC) marker that stains all ECs, both proliferating and those found in the sinusoidal blood vessels. Images were viewed using the Aperio ImageScope ver.11.2.0.780 software program for scoring analysis and assessment of signals. The positivity [Total number of positive pixels divided by total number of pixels: (NTotal – Nn)/(NTotal)] was assessed with an Aperio ScanScope (Aperio Technologies Inc., Vista, CA), ImageScope software, and an optimized algorithm (positive pixel count V9, Aperio, Inc.). Independent scoring by two people showed very high concordance for final CD31 scoring and classification (*kappa* statistic = 0.941). The presence and distribution of the number of vessels was performed by analyzing four different regions, representing the central tumour (CT), peripheral tumour (PT), adjacent normal liver (AN), and distal normal. We randomly selected three areas for each region (supplementary material, Figure S1). We scored serial sections stained with VEGFA in a similar way to CD31 staining and quantitation.

To evaluate the type of vessels, we performed double staining using CD34 and Ki67. This allowed us to identify proliferating cells and by combining this with CD34 we could quantitate new vessels and not the existing ECs in the sinusoidal blood vessels, as CD34 does not stain liver sinusoidal ECs. In addition, we stained with alpha-SMA1 to identify mature vessels, which express this antigen, compared to immature (proliferating vessels) that lack this staining. It has been demonstrated that co-opted sinusoidal blood vessels become CD34 positive when they are more central in the metastasis with RHGP [21]. Therefore we focused on the interface to evaluate proliferating vessels that stained positive for both CD34 and Ki67. In order to quantitate proliferating tumour cells, we used the Aperio Nuclear V9 Algorithm, which measures area and intensity of nuclear staining. The number of proliferating cells in addition to the intensity of staining was quantitated.

Our analysis was performed on chemonaïve, chemotherapy only, and chemotherapy + bevacizumab-treated lesions. It is important to note that the chemotherapy + bevacizumab DHGP lesions had very few to no viable tumour cells (supplementary material, Table S1) and therefore we could not quantitate the central or PT vascularity. For this reason, we quantitated the vascularity within the desmoplastic ring to characterize the type of vessels present and understand the effect of treatment.

Statistical analysis

Statistical analysis was performed with a two-tailed Fisher's exact test or a two-tailed Student's *t*-test. *P* values of <0.05 were considered to be significant.

Results

Microvessel density in CRCLM is associated with HGP

Microvessel density was evaluated by the positivity index of CD31-immunostained CRCLM tissue sections using the image analysis software ImageScope. Representative images of the CD31-immunostained CRCLM are given in Figure 1. In the RHGP CRCLMs, a high density of blood vessels can be observed, especially at the interface of the metastasis with the adjacent liver tissue (Figure 1B,D,F and supplementary material, Figure S2). At this interface, capillaries in the RHGP metastases are often in continuum with the sinusoidal blood vessels of the liver parenchyma which indicates vessel co-option as a means of vascularization (high-magnification insets of Figure 1B,D,F). In CRCLM with a DHGP, there is no morphological evidence that the capillaries connect to sinusoidal blood vessels of the adjacent liver. Instead, the capillaries in the DHGP LM connect to blood vessels of the arteriole-type, indicative of sprouting angiogenesis as a means of tumour vascularization.

Although different areas were selected for scoring (supplementary material, Figure S1), in order to assess MVD, the averages of all areas were taken and represented in Figure 2. Independent of whether

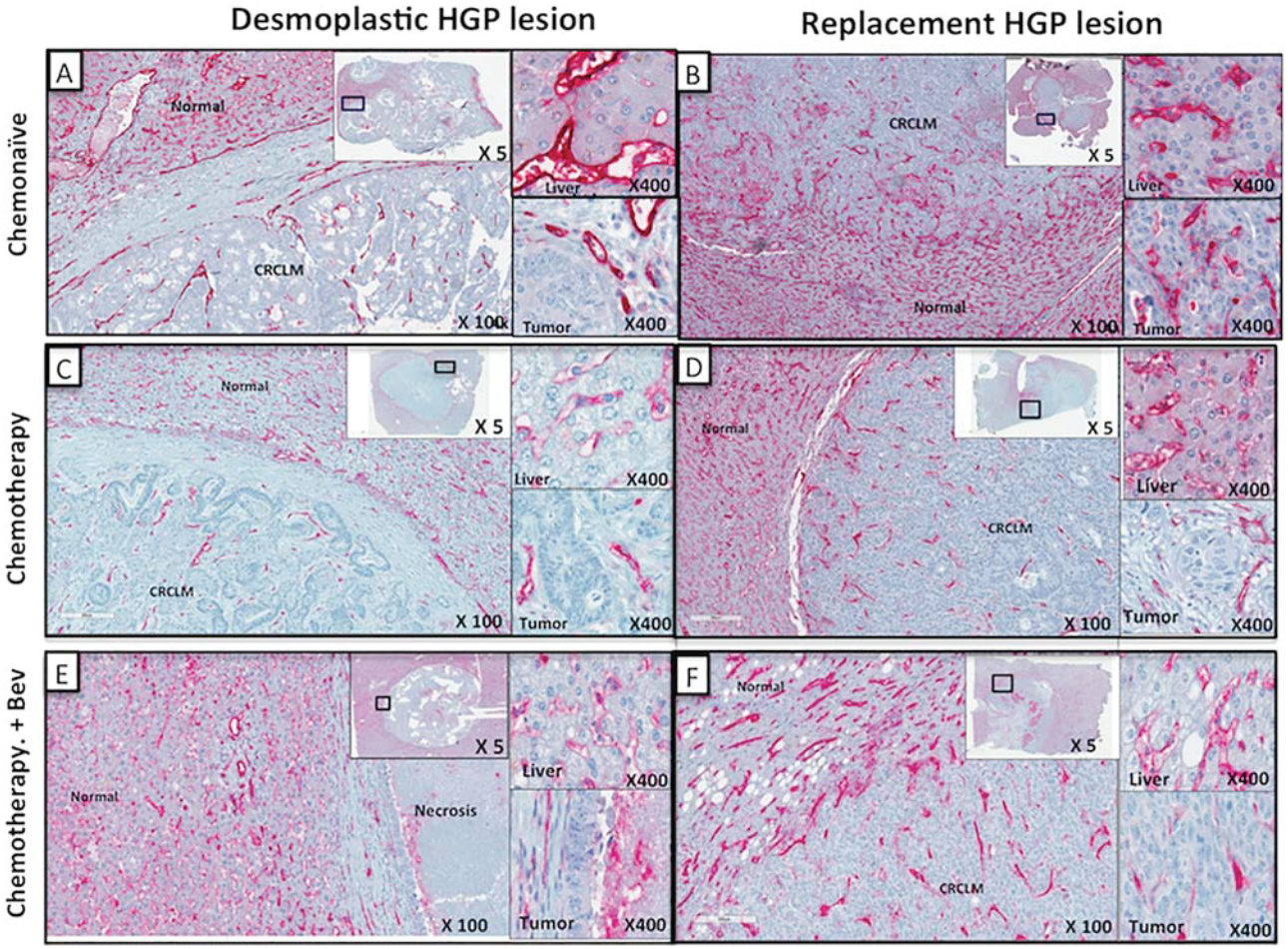

Figure 1. Microvessel density of desmoplastic histopathological growth pattern (DHGP) versus replacement histopathological growth pattern (RHGP) using CD31 Ab. Tumour sections were stained with an antibody detecting CD31, an endothelial cell marker. Representative low-magnification images of CD31 stained lesions are shown from each of the groups analyzed. Two insets are shown for each image at high magnification indicating adjacent liver staining and peripheral tumour staining. (A, C, E) DHGP lesions stained with CD31 (red): (B, D, F) RHGP lesions stained with CD31 (red). Top panels (A, B) represent chemonaïve samples; Middle panels (C, D) represent chemotherapy-treated samples; Bottom panels (E, F) represent chemotherapy + Bev-treated samples.

systemic treatment was given prior to resection, MVD was always significantly higher in CRCLMs with RHGP when compared with DHGP CRCLMs (Figure 2).

It should be noted that MVD was measured in viable tumour areas. Although there was a noticeable reduction in viable tumour cells in the group of DHGP metastases treated with chemotherapy (supplementary material, Table S1), MVD was not different when the untreated DHGP CRCLMs were compared with DHGP CRCLMs with chemotherapy prior to resection (Figure 2). There was, however, a significantly lower MVD in the group of DHGP CRCLMs that underwent combination treatment with chemotherapy and bevacizumab. This may indicate that bevacizumab is very effective at targeting angiogenesis in these lesions (supplementary material, Table S1) upon response to treatment.

In the DHGP CRCLMs with necrosis, surviving carcinoma cells were found to be present under the desmoplastic rim, which was not affected by treatment. In some cases, small RHGP areas of viable tumour grew out of these desmoplastic metastases into the liver parenchyma (Figure 3B1 and B2).

The group of RHGP metastases treated with chemotherapy before resection had a significantly lower MVD than the group of chemonaïve RHGP CRCLMs. MVD in the chemotherapy + bevacizumab group did not significantly differ from MVD in the other groups.

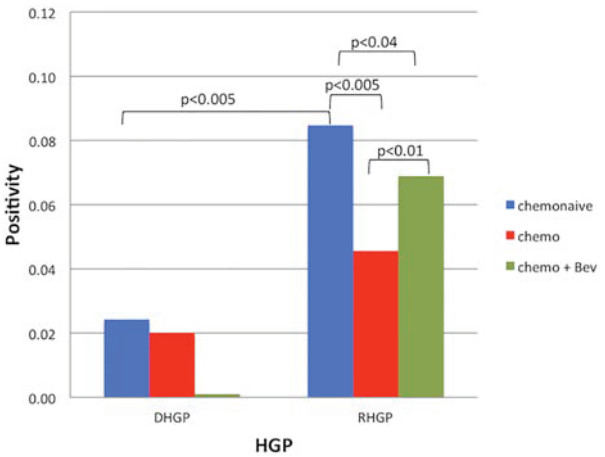

Figure 2. Quantitation of microvessel density using CD31 IHC. Quantification of CD31+ staining (three areas per tissue type: tumour versus normal) was performed using Aperio software and positive pixels were quantified and are expressed as percent positive pixels ×10 (mean + SD). Both DHGP and RHGP had the following sample sizes: Chemonaive samples: $n = 10$, Chemotherapy samples: $n = 5$, Chemotherapy + Bev samples: $n = 7$. Bev = bevacizumab.

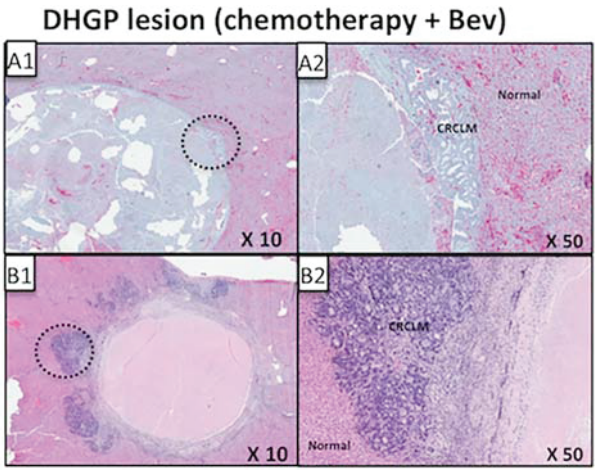

Figure 3. Replacement histopathological growth pattern (RHGP) lesions emerging from desmoplastic histopathological growth pattern (DHGP) lesions. Serial sections were stained with hematoxylin and eosin to visualize tissue architecture. (A–C) Three CRCLM DHGP lesions treated with Chemotherapy + Bev. Representative low magnifications (A1, B1, C1) and high magnifications (A2, B2, C2) are shown for designated areas. CRCLM = colorectal carcinoma liver metastasis; Bev = bevacizumab.

Moreover, no differences in the amount of necrosis were noticed when comparing the three groups of RHGP CRCLMs (supplementary material, Table S1).

DHGP lesions have a greater dependency on angiogenesis and RHGP lesions use co-option (continuity with sinusoidal network)

To assess if the vessels observed were mature (resting) or immature (proliferating), we stained serial sections with CD34/Ki67 and alpha-SMA1 (Figure 4). In the early stage of angiogenesis, the formation of new vessels has no external layer of perivascular cells and is therefore negative for alpha-SMA1. Figure 5 demonstrates the differences in the number of proliferating (CD34+/Ki67+) blood vessels in the CRCLMs. Clearly, in chemonaïve samples the DHGP metastases have a significantly ($p > 0.0005$) higher number of proliferating blood vessels than the RHGP lesions. Once the lesions are treated, we see a significant decrease in proliferating vessels in the DHGP lesions ($p > 0.0005$), however the RHGP lesions are not significantly different between the treatment groups. Since there were very few viable cells in the chemotherapy + bevacizumab-treated DHGP lesions, we could not grade the number of proliferating vessels.

When assessing the type of vessels present after treatment, the DHGP lesions have a significantly ($p < 0.05$) reduced number of proliferating blood vessels (Figures 4C,E and 5) after chemotherapy. The absence of proliferating and resting vessels after

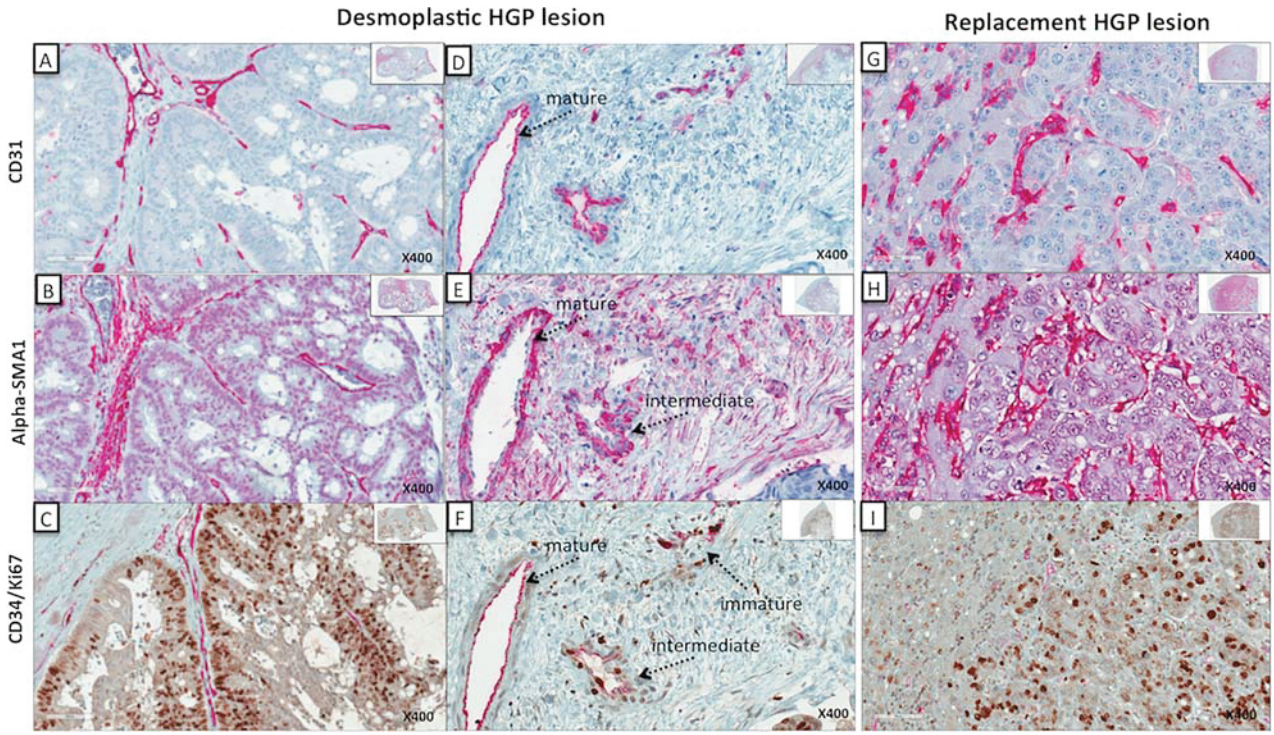

Figure 4. Identification of vessel type based on immunohistochemical staining. Chemonaïve samples demonstrating mature, and immature (proliferating) vessels. Serial sections of both RHGP and DHGP lesions are presented stained for CD31 (panels A, D, G); alpha-SMA1 (panels B, E, H); CD34 (red: endothelial cells); and Ki67 (brown: cell proliferation: (panels C, F, I). For the DHGP lesion, a higher magnification is shown demonstrating the different types of vessel. (A, D) DHGP lesions stained with CD31 (red); (G) RHGP lesion stained with CD31 (red): (B, E) DHGP lesions stained with alpha-SMA1 (red); (H) RHGP lesions stained with alpha-SMA1 (red); (C, F) DHGP lesions costained with CD34/Ki67 (red/brown); (I) RHGP lesions costained with CD34/Ki67 (red/brown).

treatment with chemotherapy + bevacizumab of DHGP lesions is due to the lack of viable tumour cells present after treatment and therefore cannot be assessed.

Current standard of care treats CRCLM patients with chemotherapy + bevacizumab. Since bevacizumab blocks the effect of VEGF-A, we stained all lesions with VEGF-A and assessed the expression between the two HGPs. Since DHGP lesions respond to treatment, one would expect that these lesions would express higher levels of VEGF-A. This was not the case. Upon staining chemonaïve samples with VEGFA, we observed no difference in expression (supplementary material, Figure S2A, B). Upon treatment, we also observed no difference in VEGF-A staining between the two HGPs (supplementary material, Figure S2C, D).

Syngeneic animal models of liver metastasis do not represent the diverse histopathological types of human liver lesions

We often compare human tissue samples with animal model samples. However, to effectively use these models, we must ensure that they resemble the human tissue. For this reason, we have characterized the vasculature of LM lesions from different metastatic animal models. It is anticipated that this approach can reveal new mechanistic understanding of basic cancer biology and be complementary to translational application of discoveries aimed at drug screening, target identification, and biomarker discovery.

When assessing H&E slides of liver lesions from the splenic injections of Lewis Lung, MC38 and CT26 cell lines into syngeneic mice, we identified the following growth patterns, respectively: 100% RHGP, 70% RHGP/30% PHGP, and 80% RHGP/20% PHGP (Figure 6A–C). To date, none of the liver metastatic models examined represent the DHGP unless we genetically modify the line as we have done in our previous work [12].

Discussion

The importance of MVD in CRC has been controversial. Correlation between a high MVD and a poor prognosis has been observed in several studies

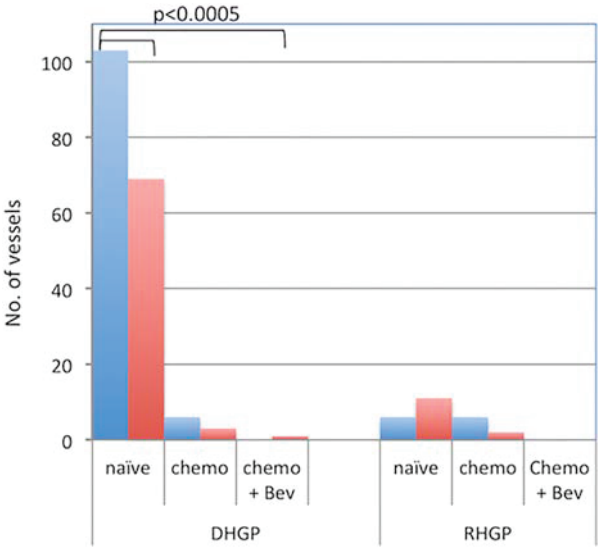

Figure 5. Quantification of vessel type based on CD34/Ki67 immunohistochemistry. Quantification of mature vessels was performed manually by counting the number of vessels that were CD34+ only. Proliferating vessels were quantitated manually by counting the number of vessels that were CD34+/Ki67+. All analysis was done using three areas within the tumour and three areas within the normal tissue by two independent people. Both DHGP and RHGP had the following sample sizes: Chemonaive samples: $n = 10$, Chemotherapy samples: $n = 5$, Chemotherapy + Bev samples: $n = 7$. Bev = bevacizumab.

[21–23] while a single study described that a high MVD correlated with a superior survival [24]. However, in those studies the MVDs of the CRCLMs were not investigated in detail in relation to lesions that responded to treatment and those that did not. Our data demonstrate that stratification of lesions based on HGP clearly shows that RHGP lesions have a higher density of vasculature than DHGP lesions, consisting of mainly nonproliferating vessels covered by pericytes. In contrast, there are significantly more proliferating vessels in DHGP than in RHGP lesions. Furthermore in chemotherapy + bevacizumab treated lesions there is only a minimal reduction in the number of vessels in RHGP lesions but there is a dramatic reduction of vessels in the DHGP lesions, which demonstrates the effectiveness of angiogenic inhibitors (AI) on DHGP lesions compared to RHGP lesions.

Our findings demonstrate that, although lesions respond differently to AIs [12] and can thus be stratified by HGP to describe this response, the lesion adopting its vasculature via co-option and not angiogenesis possibly drives the "resistance" as seen by (i) the absence of proliferating vessels in treated samples; (ii) the presence of tumour cells just under the desmoplastic ring and within the ring after treatment in the absence of proliferating vessels; and (iii) the outgrowth of tumour cells taking on a RHGP in treated samples. As RHGP lesions grow, the majority of the tumour cells are fed through the "endogenous" vasculature, via the sinusoidal capillary network, demonstrating that an invasive growth pattern that facilitates vessel co-option (RHGP) is an important and clinically relevant mechanism of resistance to anti-angiogenic therapy in CRCLM.

After analysis of 250 CRCLM cases, we have observed that patients who present with multiple lesions will have either all DHGP lesions, all RHGP lesions or, in about 10% of cases, two types of lesion, one DHGP and one RHGP (data not shown). This raises the question of what treatment would be best for these patients. Clearly, since OS is worse in RHGP patients [25] then treatment that would benefit the lesion with the worse outcome should be used. Identifying targets that could treat both HGPs remain to be elucidated.

Based on these findings, we can understand why AI effectively treats DHGPs, with their proliferating vessels, and have no or a minor effect on RHGPs,

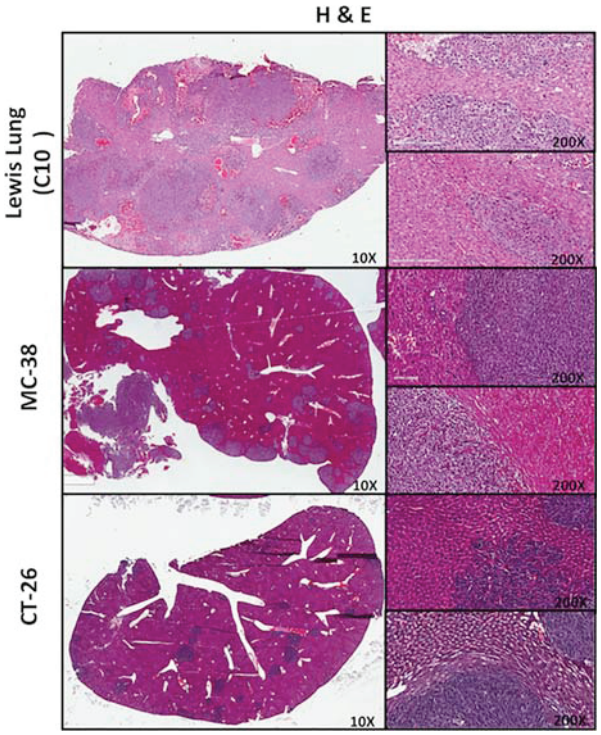

Figure 6. Characterization of mouse models of liver metastasis (Lewis Lung, MC-38 and CT-26 cell lines). Representative low-magnification images of H&E stained lesions are shown from each of the groups analyzed. Two insets are shown for each image at high magnification indicating adjacent liver and peripheral tumour.

composed of mature vessels. Surprisingly, both lesions demonstrate similar levels of VEGF-A, the target for the AI bevacizumab, staining primarily tumour cells. We speculate, based on the data, that the lack of effectiveness when RHGP lesions are treated with AIs could be from the stabilization of the vasculature, reducing leakiness and thus the chemotherapy flows through the sinusoids and has no delay time in the tumour to effectively kill the cells. This could suggest that if we increase leakiness we can more effectively deliver chemotherapy or any other drug and thus one could postulate that treating lesions with angiogenic enhancers would theoretically increase the leakiness and not affect the vasculature of the background liver since these are mature vessels and not affected by these enhancers.

Our data further show that even in lesions that are driven by angiogenesis, a subset of tumour cells survives after treatment, which utilize co-option (as seen by the absence of proliferating vessels in DHGP lesions treated with chemotherapy + bevacizumab, Figure 5), and if these lesions are not resected will grow. Adjuvant therapy using chemotherapy alone would therefore be more beneficial as the lesions left behind are driven by co-option and adding bevacizumab would have no advantage. Indeed this is the case in clinical trials where addition of bevacizumab to adjuvant chemotherapy plus systemic therapy after liver resection did not increase recurrence-free survival (RFS) or OS [26], with median RFS ($p = 0.375$) and OS ($p = 0.251$) similar in bevacizumab and no bevacizumab arms. Furthermore the combination with bevacizumab appeared to increase biliary toxicity. Studies have also suggested that neoadjuvant chemotherapy can be used to assess the responsiveness of the tumour to chemotherapy, as the initial response to chemotherapy is strongly predictive of a favorable long-term outcome [25]. Furthermore, this would explain why a higher OS is achieved in patients who are treated and resected compared to patients who are treated and not resected [12]. Additional reasons why there has been some disappointment in the efficacy of translation of preclinical results to clinical trials include: (1) a lack of appropriate preclinical tumour models and (2) a lack of endpoints of treatment and surrogate markers of response to anti-angiogenic therapy. The data presented on the metastatic animal models show that these models represent RHGP. However one must keep in mind that the mouse lesions are more aggressive, encompassing a large area of the liver and interestingly do not demonstrate the same level of inflammation or immune cells as the human samples. This suggests that the extrapolation of animal model results to human trials must be done with caution and cognizant of these shortcomings.

Histopathological features will allow us to monitor tumour type and response; however, this can only be performed on resected specimens. Dynamic imaging of tumour characteristics in response to treatment would be of significant clinical and translational value. The future lies in developing both imaging modalities and liquid biopsy biomarkers that will best identify the extent of effective and functional blood flow within a tumour vascular network and the impact of treatment on the dynamic blood supply of a tumour. By establishing these methodologies, we can then translate end-points of therapeutic response to a drug more accurately.

Acknowledgement

We thank Ana Beatriz Toledo Dias and Dr. MN Burnier for running the samples on their Ventana system.

Author contributions statement

AL designed the experiments. AA and SKP prepared the samples. AL, SKP, and AA performed tumour staining and tumour scoring. NI performed all mouse work. PZ, GZ, and PV performed all pathological evaluations and critical evaluation of the manuscript. AS consented all patients for the study. AL and PM wrote the manuscript with input and approval from all authors.

References

1. Nuttall R, Bryan S, Dale D, *et al*. Canadian Cancer Society's Advisory Committee on Cancer Statistics. *Canadian Cancer Statistics 2017*. Canadian Cancer Society: Toronto, ON, 2017. Available from cancer.ca/Canadian-Cancer-Statistics-2017-EN.pdf
2. Fernando NH, Hurwitz HI. Targeted therapy of colorectal cancer: clinical experience with bevacizumab. *Oncologist* 2004; **9:** 11–18.
3. Fusai G, Davidson BR. Strategies to increase the resectability of liver metastases from colorectal cancer. *Dig Surg* 2003; **20:** 481–496.
4. Hanahan D, Weinberg RA. Hallmarks of cancer: the next generation. *Cell* 2011; **144:** 646–674.
5. Donnem T, Hu J, Ferguson M, *et al*. Vessel co-option in primary human tumors and metastases: an obstacle to effective anti-angiogenic treatment? *Cancer Med* 2013; **2:** 427–436.
6. Rubenstein JL, Kim J, Ozawa T, *et al*. Anti-VEGF antibody treatment of glioblastoma prolongs survival but results in increased vascular cooption. *Neoplasia* 2000; **2:** 306–314.
7. Kuczynski EA, Yin M, Bar-Zion A, *et al*. Co-option of liver vessels and not sprouting angiogenesis drives acquired sorafenib

resistance in hepatocellular carcinoma. *J Natl Cancer Inst* 2016; **108:** djw030.
8. Leenders WP, Kusters B, Verrijp K, *et al*. Antiangiogenic therapy of cerebral melanoma metastases results in sustained tumor progression via vessel co-option. *Clin Cancer Res* 2004; **10:** 6222–6230.
9. Bridgeman VL, Vermeulen PB, Foo S, *et al*. Vessel co-option is common in human lung metastases and mediates resistance to anti-angiogenic therapy in preclinical lung metastasis models. *J Pathol* 2017; **241:** 362–374.
10. de Groot JF, Fuller G, Kumar AJ, *et al*. Tumor invasion after treatment of glioblastoma with bevacizumab: radiographic and pathologic correlation in humans and mice. *Neuro Oncol* 2010; **12:** 233–242.
11. di Tomaso E, Snuderl M, Kamoun WS, *et al*. Glioblastoma recurrence after cediranib therapy in patients: lack of "rebound" revascularization as mode of escape. *Cancer Res* 2011; **71:** 19–28.
12. Frentzas S, Simoneau E, Bridgeman VL, *et al*. Vessel co-option mediates resistance to anti-angiogenic therapy in liver metastases. *Nat Med* 2016; **22:** 1294–1302.
13. Vollmar B, Menger MD. The hepatic microcirculation: mechanistic contributions and therapeutic targets in liver injury and repair. *Physiol Rev* 2009; **89:** 1269–1339.
14. Vermeulen PB, Colpaert C, Salgado R, *et al*. Liver metastases from colorectal adenocarcinomas grow in three patterns with different angiogenesis and desmoplasia. *J Pathol* 2001; **195:** 336–342.
15. van Dam P-J, van der Stok EP, Teuwen L-A, *et al*. International consensus guidelines for scoring the histopathological growth patterns of liver metastasis. *Br J Cancer* 2017; **117:** 1427–1441.
16. Jass JR, Love SB, Northover JM. A new prognostic classification of rectal cancer. *Lancet* 1987; **1:** 1303–1306.
17. Terayama N, Terada T, Nakanuma Y. Histologic growth patterns of metastatic carcinomas of the liver. *Jpn J Clin Oncol* 1996; **26:** 24–29.
18. Van den Eynden GG, Bird NC, Majeed AW, *et al*. The histological growth pattern of colorectal cancer liver metastases has prognostic value. *Clin Exp Metastasis* 2012; **29:** 541–549.
19. Eefsen RL, Engelholm L, Willemoe GL, *et al*. Microvessel density and endothelial cell proliferation levels in colorectal liver metastases from patients given neo-adjuvant cytotoxic chemotherapy and bevacizumab. *Int J Cancer* 2016; **138:** 1777–1784.
20. Samani AA, Chevet E, Fallavollita L, *et al*. Loss of tumorigenicity and metastatic potential in carcinoma cells expressing the extracellular domain of the type I insulin-like growth factor receptor. *Cancer Res* 2004; **64:** 3380–3385.
21. Vermeulen PB, Van den Eynden GG, Huget P, *et al*. Prospective study of intratumoral microvessel density, p53 expression and survival in colorectal cancer. *Br J Cancer* 1999; **79:** 316–322.
22. Rajaganeshan R, Prasad R, Guillou PJ, *et al*. The influence of invasive growth pattern and microvessel density on prognosis in colorectal cancer and colorectal liver metastases. *Br J Cancer* 2007; **96:** 1112–1117.
23. Tanigawa N, Amaya H, Matsumura M, *et al*. Tumor angiogenesis and mode of metastasis in patients with colorectal cancer. *Cancer Res* 1997; **57:** 1043–1046.
24. Prall F, Gringmuth U, Nizze H, *et al*. Microvessel densities and microvascular architecture in colorectal carcinomas and their liver metastases: significant correlation of high microvessel densities with better survival. *Histopathology* 2003; **42:** 482–491.
25. Dam R, Delvart V, Pascal G, *et al*. Rescue surgery for unresectable colorectal liver metastases downstaged by chemotherapy: a model to predict long-term survival. *Ann Surg* 2004; **240:** 644–657.
26. Turan N, Benekli M, Koca D, *et al*. Adjuvant systemic chemotherapy with or without bevacizumab in patients with resected liver metastases from colorectal cancer. *Oncology* 2013; **84:** 14–21.

SUPPLEMENTARY MATERIAL ONLINE

Figure S1. Areas selected for scoring for desmoplastic histopathological growth pattern (DHGP) and replacement histopathological growth pattern (RHGP) lesions. For each lesion, we selected the following areas and annotated three areas in each: (1) Central tumour (CT: blue); (2) Peripheral tumour (PT: red); (3) Adjacent normal liver (AN: green); and (4) Distal normal liver (DN: yellow)

Figure S2. VEGF-A staining of colorectal carcinoma liver metastases (DHGP versus RHGP lesions). Tumour sections were stained with an antibody detecting VEGF-A (red). Representative low-magnification images are shown from each of the groups analyzed. Two insets are shown for each image at high magnification indicating adjacent liver staining and peripheral tumour staining. (A, C) DHGP lesions: (B, D) RHGP lesions. Top panels (A, B) represent chemonaïve samples; Bottom panels (C, D) represent chemotherapy + Bev-treated samples. Bev = bevacizumab

Table S1. Histopathological characterization of colorectal carcinoma liver metastases. Serial sections were stained with H&E to visualize tissue architecture. Viable cells, inflammation grade and necrosis are represented as percentage of total lesion. Differentiation was classified as Undifferentiated (UN) and Differentiated (D). DHGP, desmoplastic histopathological growth pattern; RHGP, replacement histopathological growth pattern (RHGP)